Modeling Ultra-Thin Flat Loop Heat Pipes using a 1-D Lumped Parameter Approach

Marco Bernagozzi[1*], Kelvin Guessi Domiciano[2], Larissa Krambeck[2], Marcia B. H. Mantelli[2], and Marco Marengo[3]

[1] *School of Architecture, Technology and Engineering, University of Brighton, Brighton, UK*
[2] *Heat Pipe Laboratory, Federal University of Santa Catarina, Florianopolis, Brazil*
[3] *University of Pavia, Pavia, Italy*
* *M.Bernagozzi3@brighton.ac.uk*

Abstract

In the present study, the transient behavior of a diffusion-bonded ultra-thin LHP, specifically designed for the thermal management of smartphones, is predicted by means of a 1-D Lumped Parameter Model (LPM). The LPM approach was previously validated for larger LHPs with different working fluids and is one of the few highly reliable transient models available in literature. The main novelty of this work is the extension of the application range of the LPM model to ultra-thin LHPs, where various parameters may affect the operation of these devices, such as heat leakage by conduction through the case material. The proposed LPM consists of a thermal network describing the thermo-fluidic behavior of the evaporator, connected to a series of mass, momentum, and energy conservation, solved iteratively to predict the device temperatures, heat transfer rates, and thermal resistances. The LPM model successfully predicted the transient temperature of the LHP with the highest and lowest average difference of 0.99 °C and 1.65 °C, respectively. Also, this approach estimated the steady-state thermal resistance with an average discrepancy of 28%. Therefore, the LPM showed to be a powerful design tool to predict and simulate the operation conditions of heat pipes, from ultra-thin to larger ones.

Keywords: Flat Loop Heat Pipe; Lumped Parameter Model; Transient Modelling; Diffusion Bonding; Thermal performance.

1. Introduction

Lightweight, compactness and high performance are the requirements for thermal management of electronic gadgets. Flat Loop Heat Pipes (LHPs) are suitable passive cooling solutions as they can separate the evaporator from the condenser section, optimizing the integration to the electronic devices. Moreover, the LHPs can be miniaturized, reducing the final thickness of electronics [1].

Investigation on novel manufacturing method for LHP have been object of interesting research over the last few years, and amongst those diffusion bonding has been proven to be an extremely effective manufacturing technique for producing flat heat pipes [2, 3]. Domiciano et al. [3] developed a diffusion-bonded ultra-thin LHP for small electronic gadgets, like smartphones and tablets, which validated the fabricating method and resulted in a device with excellent thermal performance under natural convection as a heat sink.

Despite the recent technical progress in heat pipe manufacturing, their adoption from industry is still limited, mainly due to the uncertainty on predicting their behaviour and the lack of a design tool. This is where numerical simulations methods offering accurate results in short computational time become greatly appealing. Prime example of this is the Lumped Parameter Modelling, where continuous complex geometries are broken down and assigned into discrete components, called nodes.

Applying this approach to a LHP means dividing it into discrete components like the evaporator, condenser, vapor, and liquid lines. The governing equations based on mass, momentum, and energy conservation are solved iteratively to predict key performance parameters like operating temperatures, heat transfer rates, and thermal resistances.

In the present work, a previously validated 1-D Lumped Parameter Model (LPM) for thermodynamic simulation of large-scale LHPs is used to predict the thermal performance of an ultra-thin flat LHP, designed for electronics cooling applications, especially smartphones. As the compactness of these two-phase devices affects the heat conduction by the wick structure and case material, this heat leakage became crucial for modeling ultra-thin LHPs. The proposed model is used to replicate the experimental results reported by Domiciano et al. [3]. Therefore, the main aim of this research is to understand if the envelope of this LPM can be pushed to successfully simulate and predict the thermal performance of ultra-thin LHPs.

2. Studied LHP

The studied LHP was manufactured by diffusion bonding of three copper sheets. The total thickness of this device is 1.56 mm, given by two external sheets of 0.3 mm and one internal structure 1.0 mm thick. The flat LHP container was divided into four sections, as shown in Figure 1, which are the evaporator, vapor line, condenser, and vapor line. Due to the compactness requirements of the proposed device, the compensation chamber was suppressed.

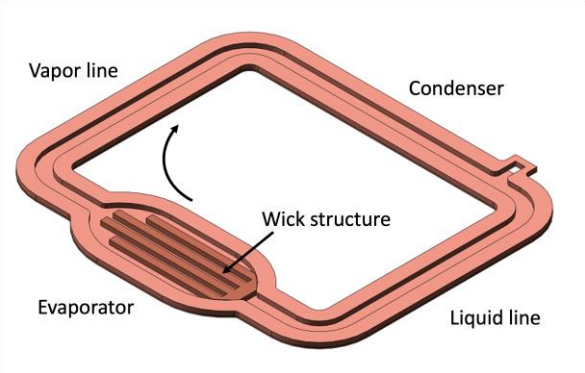

Figure 1. Design of the ultra-thin LHP.

The evaporator contains a wick structure made by the sintering process of a copper powder. Its geometry improves the evaporation of the working fluid and guarantees a single direction of the loop, given by a vapor barrier on the liquid line side. The main properties of the sintered copper powder is shown in Table 1.

The diffusion bonding consisted of submitting the pilled copper sheets, with the sintered powder wick, into a pressure system made by screws and a matrix, followed by a thermal process in a furnace (Jung® LT1513) at 875 °C for one hour. An atmosphere of argon (95%) and hydrogen (5%) inside the furnace reduced corrosion effects. More details about the applied diffusion bonding procedure can be found in Domiciano et al. [3]. The sintering powder process was the same as the diffusion bonding, without the pressure application. In the end, a capillary tube was brazed to the container, and a leakage test was performed.

Ethanol was selected as the working fluid with the filling ratio (FR) that provided the best thermal performance, which corresponds to an FR of 30 %, according to previous tests [3]. FR is defined as the total volume of working fluid divided by the total internal void volume. Table 1 presents the main features of the resulting LHP.

Table 1. Main characteristics of developed LHP.

Component	Characteristic
Total dimensions [mm^3]	76 x 60 x 1.56
Evaporator area [mm^2]	37.5 x 20
Evaporator active area [mm^2]	10 x 10
Evaporator wick area [mm^2]	29 x 1.5
Vapor grooves area [mm^2]	23.5 x 1.3
Vapor line channel area [mm^2]	79.17 x 3
Liquid line channel area [mm^2]	79.17 x 3
Condenser area [mm^2]	46 x 3
Working fluid	Ethanol
Filling ratio [%]	30
Volume [ml]	0.26
Particle average diameter [µm]	49.72 [4]
Porosity [%]	53.46 ± 3.87 [4]
Permeability [10^{-12} m^2]	1.99 ± 1.02 [5]
Effective porous radius [µm]	21.04 ± 2.2 [6]

For the experimental test, a workbench, schematized in Figure 2, mimicked the power input of a typical electronic chip, using a cartridge electrical resistor. The resistor was embedded in a copper block (1 cm^2 of contact area) and attached to the outer surface of the evaporator, supplied by a power energy system (TDK-Lambda® GEN300-5). The contact resistance was reduced by thermal grease. Natural convection removed the excess heat in the condenser section, in which the environment was kept at 24 ± 1 °C. Also, the evaporator was insulated with PTFE polymer (Polytetrafluoroethylene), minimizing the heat loss to the environment.

A data acquisition system (DAQ-NI® SCXI-1000), a laptop (Dell®), and T-type thermocouples (Omega Engineering®) acquired temperature measurements. Six thermocouples were fixed at the external surface, according to the positions presented in Figure 2, using thermosensitive adhesive strip Kapton®. Also, the environment temperature was measured during the test.

The LHP was tested in gravity-assisted orientation, meaning the evaporator was below the condenser. Heat loads were applied from 0.5 to 8 W for 1200 seconds each, guaranteeing steady-state conditions (temperature variation lower than 0.1 °C/min). Data was acquired every one second.

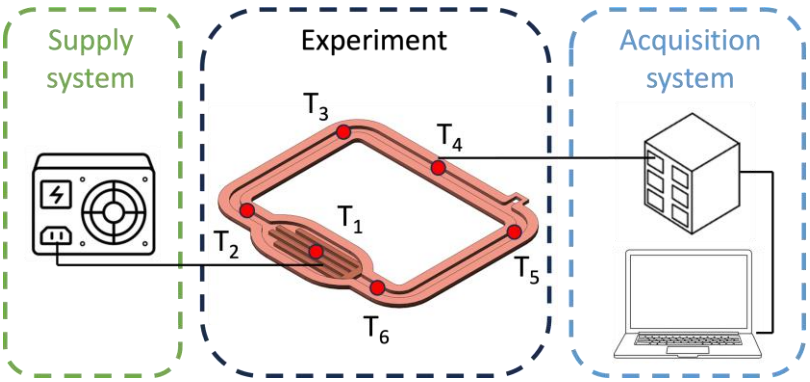

Figure 2. Experimental apparatus.

The LHP thermal performance was evaluated by the overall thermal resistance, R_{exp}, estimated by:

$$R_{\exp} = \frac{T_1 - T_4}{q} \quad (1)$$

where T_1 is the evaporator temperature, T_4 is the temperature measurement in the middle of the condenser, and q is the heat load, given by the current times the voltage.

A calibration procedure was performed in the entire experimental workbench to reduce the errors related to the temperature measurements. The overall thermal resistance uncertainty, δR_{exp}, was calculated by:

$$\delta(R_{\exp})^2 = \left[\frac{\partial R}{\partial T_1}\delta T_1\right]^2 + \left[\frac{\partial R}{\partial T_4}\delta T_4\right]^2 + \left[\frac{\partial R}{\partial q}\delta q\right]^2 \quad (2)$$

where this expression includes the uncertainties of the thermocouples, data acquisition system, and power supply unit, determined by the error propagation technique according to Holman [7]. After the calibration, the maximum temperature uncertainty was 0.21 °C.

3. Lumped Parameter Model

The LPM model used in this work is taken from the validated works by Bernagozzi et al. [8] [9], which have been successfully validated with different LHP layout (flat plate and cylindrical) and different working fluids (R123, ammonia, water, ethanol and Novec 649©).

The principal modifications of the LPM for the present ultra-thin device are the absence of the compensation chamber and the working fluid confinement, induced by the thickness reduction, increasing the heat leak from the evaporator to the liquid line.

A schematic design of the thermal network, which was modified for the proposed ultra-thin LHP, can be seen in **Error! Reference source not found.**a. Compared to previous works [8] and [9], the compensation chamber was removed from the thermal network. Experimental data from [3] were used: the average heat transfer coefficient by natural air convection in the condenser (30.4 W/m^{2}K), the working fluid mass flow rates, and the average experimental heat leakage from the evaporator to the environment through the insulation (15.46%).

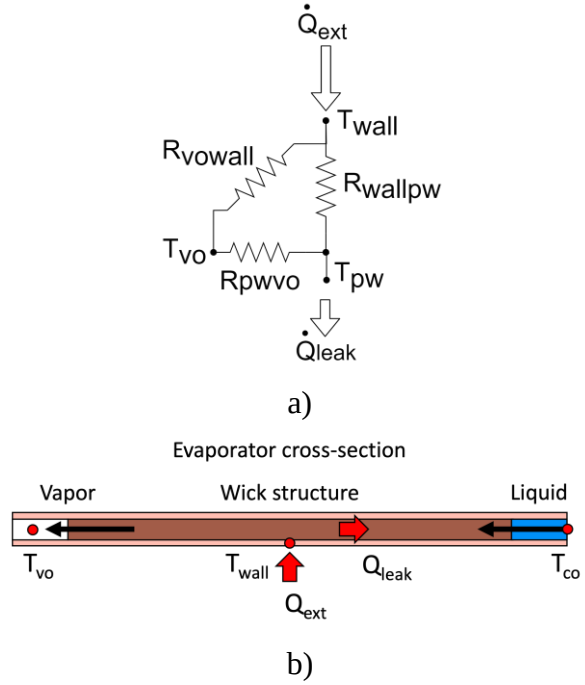

Figure 3. Flat Plate LHP evaporator a) thermal network and b) schematic for reference. wall: evaporator wall; vo: vapour outlet – exiting the

evaporator; co – condenser outlet – all the condenser section and liquid line are subjected to the same external heat transfer coefficient hence considered as condenser.

Error! Reference source not found.b shows the actual location of the temperature estimations from the proposed model. As mentioned, heat is applied in the external surface (Q_{ext}) of the evaporator, where the temperature of this region is given by T_{wall}. In the sequence, heat is transferred to the working fluid, resulting in its evaporation and leaving the evaporator with T_{vo}. However, due to the wall and wick structure material, a fraction of the total heat leaks the liquid line section, which does not contribute to the evaporation of the working fluid (Q_{leak}). Vapor starts to condense while flows in the condenser section. The condensed liquid exits the condenser with T_{co}, flowing back to the evaporator from the condenser through the liquid line, closing the loop. It is worth to mention that, since both the condenser and the liquid line are subjected to the same external heat transfer conditions, they are both treated as condenser in the model.

Error! Reference source not found.a displays the thermal network associated to the evaporator which instructed the writing of the main ODE system, presented in Eqs. (3-5). The first one, the evaporator wall node, is expressed as follows:

$$\dot{m}_{wall} c_{p,wall} \frac{dT_{wall}}{dt} = \frac{T_{vo} - T_{wall}}{R_{vowall}} + \frac{T_{co} - T_{wall}}{R_{wallco}} + \dot{Q}_{ext} \quad (3)$$

where $\dot{m}_{wall}$ is the mass flow rate in this node, $c_{p,wall}$ is the specific heat of the evaporator wall and R_{vowall} and R_{wallco} are the thermal resistance between T_{wall} and T_{co}, and between T_{wall} and T_{co}, respectively.

The second node is in the vapor channels, where vapor leaves from the evaporator. The governing equation of this element is:

$$\dot{m}_{vo} c_{p,v} \frac{dT_{vo}}{dt} = \frac{T_{co} - T_{vo}}{R_{covo}} + \frac{T_{wall} - T_{vo}}{R_{vowall}} + \dot{m} c_{p,v} (T_{sat} - T_{vo}) \quad (4)$$

where $\dot{m}_{vo}$ is the vapour mass flow rate generated by boiling, $c_{p,v}$ is the specific heat of the vapor phase and R_{covo} and R_{vowall} are the thermal resistance between T_{co}, and T_{vo} and between T_{vo} and T_{wall}, respectively. The last element of Eq. (4) accounts for the vapour superheat.

The last node is in the end of the condensing section, where vapor enters the inlet section and leaves as a liquid. Therefore, the following equation expresses the transient behavior in this node:

$$\dot{m}_{co} c_{p,co} \frac{dT_{co}}{dt} = \frac{T_{vo} - T_{co}}{R_{covo}} + \frac{T_{wall} - T_{vo}}{R_{vowall}} - \dot{m} c_{p,l} (T_{co} - T_{ll}) - \dot{Q}_{leak} \quad (5)$$

where $\dot{m}_{co}$ is the liquid mass flow rate returning to the evaporator and $c_{p,l}$ is the specific heat of the liquid phase. The second to last element of Eq. (5) accounts for the subcooling coming from the liquid line.

Besides these expressions, another governing equation related to the heat leakage from the evaporator to the liquid line due to the temperature difference between these two regions is used, which is crucial for the operating of compact two-phase devices. Thus, there is an increase in the temperature of the liquid line given by this heat leakage ($\dot{Q}_{leak}$), which can be assessed with the following expression:

$$T_{co} = T_{ll} + \frac{\dot{Q}_{leak}}{\dot{m} c_{p,l}} \quad (6)$$

where T_{ll} is the last node of the liquid line.

Lastly, the LPM model can evaluate the steady-state thermal resistance (R_{num}) with the following expression:

$$R_{num} = \frac{T_e - T_c}{q} \quad (7)$$

where T_e is the evaporator temperature given by T_{wall} and T_c is the condenser temperature that can be assessed by the average temperature between T_{vo} and T_{co}.

4. Results and discussion

4.1. Experimental results

In order for the ultra-thin LHP to start its operation as a two-phase device, a pressure difference between the evaporator and the condenser must exist, given by the temperature variation in these regions. Therefore, with the wick structure of the LHP fully saturated with liquid, when heat is applied to the outer surface of the evaporator, its temperature increases, generating vapor. The resulting vapor flows in the direction of the condenser, condensing it up to some fraction of

the condenser. Assisted by the capillary and vapor pressure, the condensate returns to the evaporator. Thus, in this paper, the startup can be considered when vapor reaches the condenser section, increasing its temperature (T_4 in Figure 2).

Figure 4 shows the temperature distribution of the ultra-thin flat LHP operating in the gravity-assisted orientation under several heat loads. With the increase of the power input, the steady-state temperature of each power level increased. The startup of LHP occurred at 2 W, when the condenser temperature (T_4) increased and overlapped the inlet evaporator temperature (T_6). For the LHP startup, an evaporator temperature of 43.36 °C and a temperature difference between the evaporator and condenser of 1.63 °C was necessary.

From Figure 4, above 4 W, all temperatures of the condenser section (T_3, T_4 and T_5) were kept at almost the same level, meaning that at this heat load, the entire condenser area was being used for the condensation of the working fluid.

The maximum heat flux dissipated by the LHP, without reaching the established limit temperature of 100 °C, was 8 W, with an evaporator temperature of 90.6 °C. No dry-out condition was observed, which means that the LHP could transfer higher heat fluxes; however, with a higher evaporator temperature.

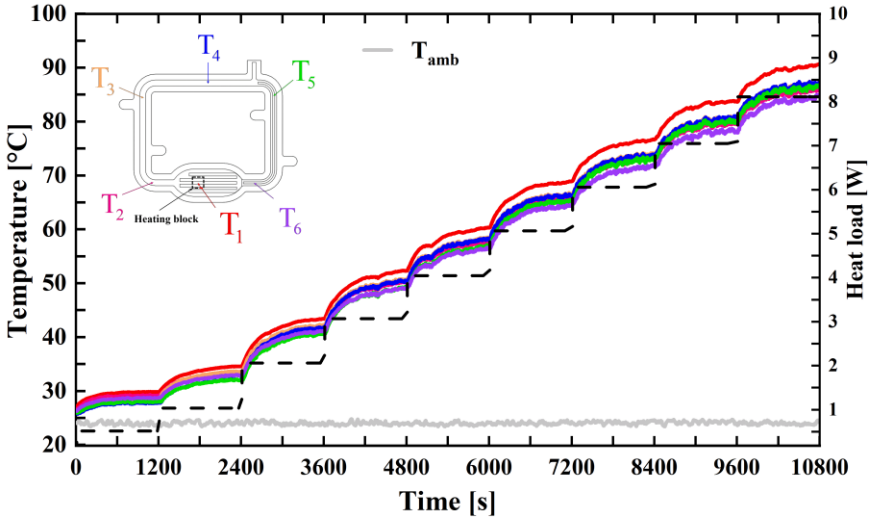

Figure 4. Temperature distribution of ultra-thin flat LHP operating in the gravity-assisted orientation [3].

4.1. Numerical results

Figure 5 presents the transient temperatures along the LHP given by the experimental data and numerical results. The dashed grey line shows the experimental results from [3], while the solid black line illustrates the numerical data obtained with the present LPM. In Figure 5a, T_{wall} is the evaporator temperature measured by T_1. In Figure 5b, T_{vo} is the evaporator outlet temperature obtained by T_2. In Figure 5c, T_{co} is the condenser exit temperature provided by T_5.

In Figure 5a, from 0.5 to 2 W, both numerical and experimental lines present an excellent match, both in terms of steady state values and trends. Above 2 W, a discrepancy at the end of the steady state section starts to appear, with the numerical model underpredicting the experimental data. However, both data still show satisfactory agreement, with an average difference between the evaporator temperature (T_1) and the numerical evaporator temperature ($T_{wall,num}$) of 0.99 °C.

For the evaporator outlet temperature, Figure 5b shows good agreement between the numerical and experimental data for all applied heat loads, with the exception of 8 W. In this case, the average difference between both temperatures (experimental and numerical) was 1.20 °C.

The last comparison presented is the condenser outlet temperature. From Figure 5c, some minor differences can be seen in all heat loads, in which the numerical data presents lower temperatures up to 2 W and higher from 5 W to 8 W. The comparison of this case showed the highest discrepancy between the numerical and experimental temperatures, 1.65 °C.

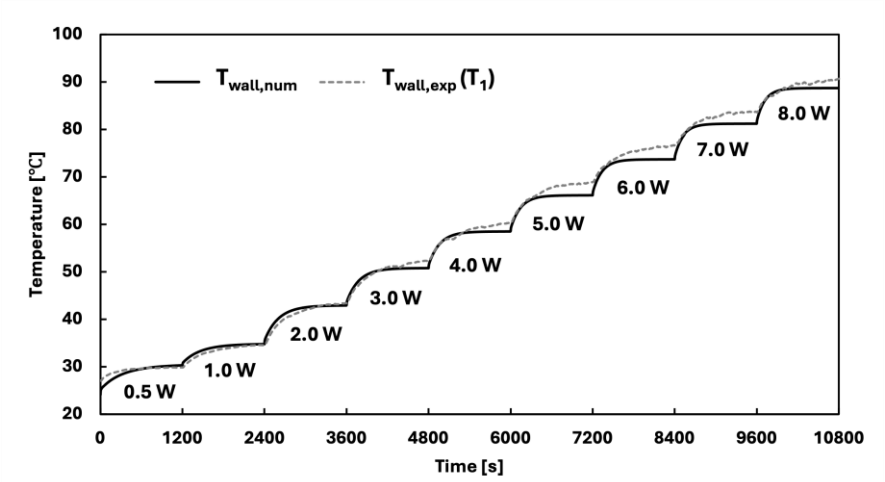

(a)

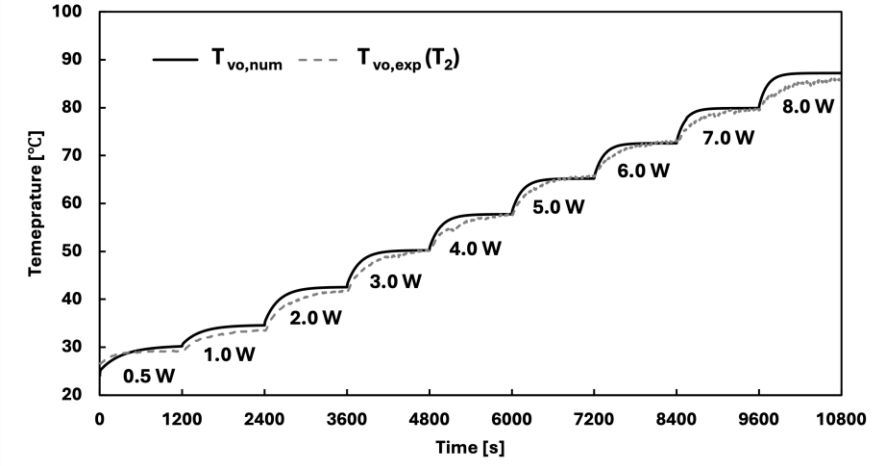

(b)

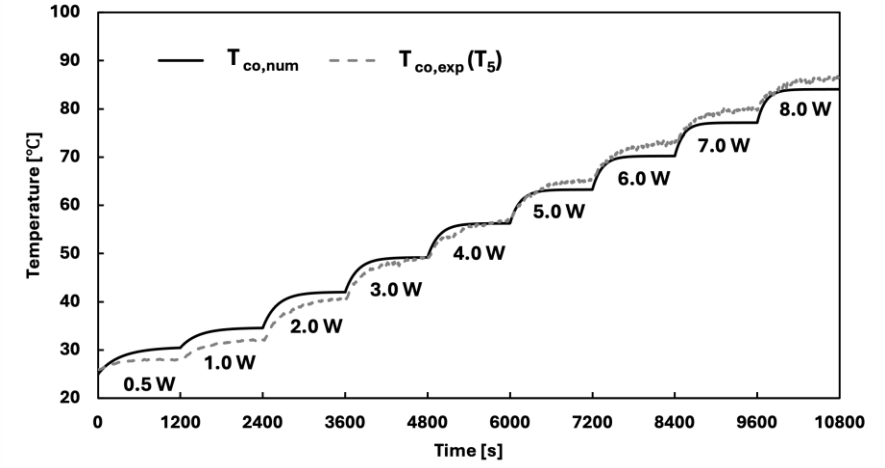

(c)

Figure 5. Comparison of the experimental and numerical transient temperatures along the LHP (a) evaporator wall, (b) evaporator exit, and (c) condenser outlet.

Figure 6 shows the comparison between the experimental (black round dots) thermal resistance, given by Eq. (1), and the numerical (grey line) thermal resistance obtained by Eq. (7). The thermal resistance of the proposed LHP without working fluid inside, i.e., transferring heat only by heat conduction, was 3.33 ± 0.43 °C/W. From Figure 6, it is clear that the LHP startup at 2 W, as mentioned in Figure 4, with an abrupt decrease in its thermal resistance. Above 2 W, the thermal resistance

remained at an almost constant level, reaching the minimum value of 0.4 °C/W at 7 W.

Since the proposed LPM model only considers the LHP operating as a two-phase device, the comparison of the numerical and experimental results accounts only heat loads from 2 W to 8 W, where the LHP properly operates. Considering this range of operation, the numerical model could successfully predict the thermal resistance of the proposed LHP, presenting an average discrepancy of 28%.

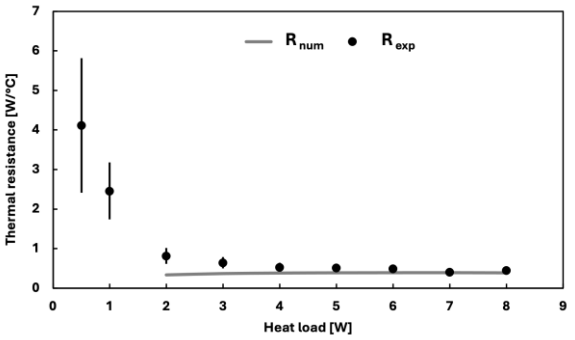

Figure 6. Comparison between the numerical and the experimental thermal resistance.

From the presented results, the proposed LPM model could successfully simulate and predict the transient temperature of the LHP for all applied heat loads, including those where the LHP was not operating as a two-phase device. Considering the thermal resistance, the LPM model reasonably estimated it, but improvements can be made, especially in simulating the condenser section temperature; however, only for the heat loads where the LHP was operating in two-phase mode.

In this context, in general, the proposed LPM showed to be a successful tool for the transient thermal performance prediction of an ultra-thin LHP.

5. Conclusions

In the present work, a previously studied 1-D lumped parameter model, already validated for larger LHPs and different working fluids, is proposed for predicting the transient thermal behavior of an ultra-thin LHP specially designed for smartphones. The main goal of this research was to understand the applicability of the 1-D LPM for ultra-thin two-phase devices. The results have shown that:

a. The proposed LHP properly operated in the gravity-assisted mode, starting at 2 W up to 8 W with a minimum thermal resistance of 0.4 °C/W at 7 W.
b. The proposed 1-D LPM can successfully simulate and predict the transient temperature and thermal resistance of a ultra-thin LHP of 1.56 mm of total thickness if the heat leakage from the evaporator to the liquid line is considered.
c. The transient behavior of the LHP can be predicted by estimating three temperatures along the LHP: the evaporator, the outlet evaporator, and the condenser exit. Comparing these results with the experimental data, an average temperature difference between these results of 0.99 °C, 1.20 °C, and 1.65 °C, respectively, were obtained.
d. The 1-D LPM model predicted the steady-state thermal resistance with an average discrepancy of 28% for the heat loads in which the LHP was able to operate as a two-phase device.

Finally, the present research showed the possibility of using the 1-D LPM for ultra-thin LHPs operating in the gravity-assisted mode with ethanol as the working fluid. In future works, new operation conditions and different working fluids must be accomplished in order to improve the proposed model as design tool for new ultra-thin two-phase devices. Furthermore, this model can be used to compute the combined effect of thermal resistance, density of the device and its thickness, which is one of the most important parameters for the thermal management of smartphones or microelectronics, to compare it with other standard technologies.

6. Acknowledgements

The authors acknowledge the National Council for Scientific and Technological Development (CNPq), National Fund for Scientific and Technological Development (FNDCT), and Ministry of Science, Technology, and Innovations (MCTI) for funding the projects: 405784/2022-8 and 406451/2021-4, and the scholarship of the second author, under grant number 381267/2023-7. The authors also acknowledge the Foundation for Research Support of Santa Catarina (FAPESC) for providing a scholarship for the first author under grant number 3003/2021. Also, acknowledgments are offered to the Graduate Program in Mechanical Engineering of UFSC, which funded the congress participation of the research team. Finally, the Authors would like to thank the School of

Architecture, Technology and Engineering at the University of Brighton for the economic support.

References

[1] H. Tang, Y. Tang, Z. Wan, et al., Review of applications and developments of ultra-thin micro heat pipes for electronic cooling, Applied Energy. 2018, 223 (April): pp. 383–400.

[2] K.G. Domiciano, L. Krambeck, J.P.F. Mera, and M.B.H. Mantelli, Study of a new thin flat loop heat pipe for electronics, Heat and Mass Transfer/Waerme- und Stoffuebertragung. 2023, (0123456789): p.

[3] K.G. Domiciano, L. Krambeck, J.P.M. Floréz, and M.B.H. Mantelli, Thin diffusion bonded flat loop heat pipes for electronics : Fabrication , modelling and testing, Energy Conversion and Management. 2022, 255 (November 2021): p.

[4] J.P.M. Florez, M.B.H. Mantelli, G.G.V. Nuernberg, and F.H. Milanez, Powder Geometry based models for sintered media porosity and effective thermal conductivity, Journal of Thermophysics and Heat Transfer. 2014, 28 (3): pp. 507–517.

[5] J.P. Flórez Mera, M.E. Chiamulera, and M.B.H. Mantelli, Permeability model of sintered porous media: analysis and experiments, Heat and Mass Transfer/Waerme- und Stoffuebertragung. 2017, 53 (11): pp. 3277–3285.

[6] J.P.F. Mera, Heat and Mass Transfer Analysis of a Copper Loop, (2016).

[7] J.P. Holman, Experimental methods for engineers. , New York, USA, 2011.

[8] M. Bernagozzi, A. Georgoulas, N. Miché, C. Rouaud, and M. Marengo, Novel battery thermal management system for electric vehicles with a loop heat pipe and graphite sheet inserts, Applied Thermal Engineering. 2021, 194 p.

[9] M. Bernagozzi, S. Charmer, A. Georgoulas, I. Malavasi, N. Michè, and M. Marengo, Lumped parameter network simulation of a Loop Heat Pipe for energy management systems in full electric vehicles, Applied Thermal Engineering. 2018, 141 pp. 617–629.